EPJ Photovoltaics **3**, 35003 (2012)
www.epj-pv.org
DOI: 10.1051/epjpv/2012006

Effect of annealing on properties of sputtered and nitrogen-implanted ZnO:Ga thin films

K.S. Shtereva[1,2,a], V. Tvarozek[1], I. Novotny[1], P. Sutta[3], M. Milosavljevic[4], A. Vincze[5], M. Vojs[1], and S. Flickyngerova[1]

[1] Institute of Electronics and Photonics, Slovak University of Technology, Ilkovicova 381219 Bratislava, Slovakia
[2] Department of Electronics, University of Rousse, Studentska 8, 7017 Ruse, Bulgaria
[3] New technologies-Research Center, University of West Bohemia, Plzen Czech Republic
[4] VINČA Institute of Nuclear Sciences, Laboratory for Atomic Physics, Belgrade, Serbia
[5] International Laser Centre, Bratislava, Slovakia

Received: 14 July 2011 / Accepted: 18 April 2012
Published online: 12 July 2012

Abstract Thin films of gallium-doped zinc oxide (ZnO:Ga) were deposited on Corning glass substrates by rf diode sputtering and then implanted with 180 keV nitrogen ions in the dose range of $1\times10^{15} \div 2\times10^{16}$ cm^{-2}. After the ion implantation, the films were annealed under oxygen and nitrogen ambient, at different temperatures and time, and the effect on their microstructure, type and range of conductivity, and optical properties was investigated. Post-implantation annealing at 550 °C resulted in *n*-type conductivity films with the highest electron concentration of 1.4×10^{20} cm^{-3}. It was found that the annealing parameters had a profound impact on the film's properties. A *p*-type conductivity (a hole concentration of 2.8×10^{19} cm^{-3}, mobility of 0.6 cm^2/V s) was observed in a sample implanted with 1×10^{16} cm^{-2} after a rapid thermal annealing (RTA) in N_2 at 400 °C. Optical transmittance of all films was >84% in the wavelength range of 390–1100 nm. The SIMS depth profile of the complex $^{30}NO^-$ ions reproduces well a Gaussian profile of ion implantation. XRD patterns reveal a polycrystalline structure of N-implanted ZnO:Ga films with a *c*-axis preferred orientation of the crystallites. Depending on the annealing conditions, the estimated crystallite size increased $25 \div 42$ nm and average micro-strains decreased $1.19\times10^{-2} \div 6.5\times10^{-3}$ respectively.

1 Introduction

At present, impurity-doped ZnO thin films with high conductivity and transparency are used as an electrode material for amorphous silicon (a-Si) and Cu(In, Ga)Se_2 (CIGS) photovoltaic devices (PV), and have been investigated for electrodes for organic PV and organic light-emitting diodes (OLEDs) [1, 2]. A ZnO semiconductor (a wide direct band gap of 3.37 eV at room temperature and a large exciton binding energy of 60 meV) has the potential to create new transparent electronics products, such as transparent thin film transistors (TTFT) and light-emitting diodes (LED) [3]. The major obstacle to ZnO device applications is the impossibility for controllable and reproducible *p*-type doping. Main reasons of failure to dope ZnO *p*-type are: (1) the low or limited solubility of the acceptor dopants; (2) the high activation energies of these dopants; (3) the tendency to form spontaneously compensating defects; and (4) hydrogen or other impurities, acting as unintentional extrinsic donors in ZnO. Among others, nitrogen has been investigated as a promising acceptor dopant and a number of groups, including ours, reported *p*-type conductivity in nitrogen-doped ZnO films (ZnO:N) [4, 5]. The use of ion implantation to dope semiconductors has become increasingly important. In comparison to diffusion, ion implantation offers the precise process control (doping levels and doping uniformity, extreme purity of the dopant) and therefore, has been used for device fabrication. Moreover, ion implantation enables the introduction of dopants that are not soluble or diffusible, and hence, provides better opportunities for *p*-type doping in ZnO. Although there were few reports on *p*-type doping in ZnO via nitrogen implantation [6,7], more studies are needed to understand phenomena and optimize parameters of the ion implantation processing (energy, dose). Implantation causes damage and disorder that have to be annealed to improve the material quality. Therefore, the right choice of post-implantation annealing parameters (ambient, temperature, time), is an important step to prepare a good quality material.

In this work we investigated influence of the post-implantation annealing parameters (ambient, temperature, time), on the physical properties of sputtered N-implanted ZnO:Ga thin films, and the possibility for *p*-type doping.

[a] e-mail: KShtereva@ecs.uni-ruse.bg

2 Experimental methods

In this study were used ZnO:Ga thin films deposited on Corning 7059 (a baria alumina borosilicate composition, an alkali level of <0.3%) glass substrates by rf diode sputtering from a ceramic ZnO:Ga_2O_3 (98 wt%:2 wt%) target, a mixture of ZnO (99.99% purity) and Ga_2O_3 (99.99% purity). The film thickness of ∼500 nm was determined by Dektak 150 instrument. The ZnO:Ga films were *n*-type conductivity with the highest electron concentration of 7.2×10^{19} cm^{-3} and mobility of ∼1.2 cm^2/V s measured from a Hall-effect system with a magnetic field of 0.15 T at a room temperature (RT). Nitrogen ions were implanted at 180 keV under normal incidence into the sputtered ZnO:Ga films with doses of 1×10^{15}, 5×10^{15}, 1×10^{16} and 2×10^{16} cm^{-2}. Prior to implantation, the theoretical nitrogen profiles were calculated by means of Monte Carlo simulations using the SRIM code for the various doses [8]. The projected range (R_P) at 180 keV was determined to be 340 nm. Post-implantation annealing was done under an oxygen (O_2) (at 550 °C for 30 min) and nitrogen (N_2) (at 400 and 550 °C for 10 s) ambient. The structure and preferred orientation of crystallites were evaluated by X-ray diffraction (XRD) on X'pert Pro powder diffractometer (symmetric ϑ-ϑ geometry) equipped with an ultra-fast linear semiconductor detector PIXcel using CuKα radiation ($\lambda = 0.154$ nm). Secondary ion mass spectrometry (SIMS) depth profiles of the various ionic species were acquired with a TOF-SIMS IV analyzer, product of ION TOF GmbH, Muenster, using a Cs^+ primary ion beam with energy of 2 keV. Optical spectrophotometry measurements were carried out from the UV region to the near IR region by an Ava Spec-2048 Fiber Optic Spectrometer.

3 Results and discussions

All non-implanted ZnO:Ga films showed a *c*-axis preferred orientation of crystallites with a dominant (002) diffraction line at $2\theta = 34.29°$, and weak lines at 2θ of 31.53° and 35.76° that corresponds to (100) and (101) crystal planes of ZnO. They were *n*-type conductivity with quite uniform parameters, an electron concentration in the range of $5 \times 10^{19} \div 7.2 \times 10^{19}$ cm^{-3}, mobility of $1.2 \div 1.6$ cm^2/V s and resistivity of $7.6 \times 10^{-2} \div 7.8 \times 10^{-2}$ Ω cm.

The resistivity of the films increased and the carrier concentration decreased after nitrogen implantation. The higher resistivity in implanted samples can be explained with: (1) nitrogen introduction and formation of N_O acceptors that partly compensate donor defects in the film, and (2) the damage caused by ion implantation. Some support for this first assumption is the unstable *p*-type conductivity in some samples implanted with low nitrogen doses before annealing. It indicates that the implanted nitrogen produces holes which compensate electrons, and hence the carrier concentration is reduced. Calculations based on the first-principles pseudo potential method within the local-density functional approximation (LDA) show that the type of the donors that compensate nitrogen acceptors depends on the nitrogen doping level and the type of the nitrogen source [9]. At low nitrogen doping levels, nitrogen acceptors are compensated mostly by oxygen vacancies, whereas at high doping levels, the major compensating donors are nitrogen composed donors. Hence, *n*-type conductivity in samples implanted with high nitrogen doses can be explained with self-compensation of the N_O acceptors by nitrogen composed donors, such as nitrogen molecules and donor defect complexes. Furthermore, implantation of high nitrogen doses can introduce a considerable amount of nitrogen interstitials in the film that may become a source of electrons as well as holes. During implantation, N^+ ions penetrate the sample with high energy. Their collisions with the native atoms can displace some of these atoms and thus provide additional donor defects.

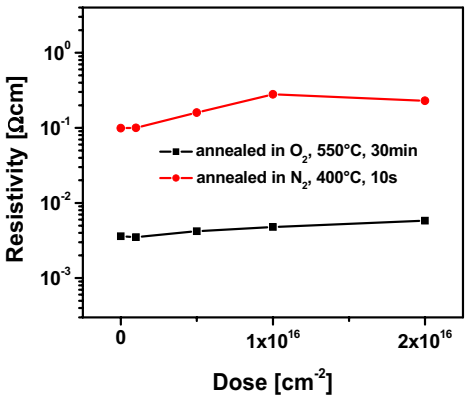

Fig. 1. Resistivity of N-implanted ZnO:Ga films, annealed in O_2 at 550 °C for 30 min, and in N_2 at 400 °C for 10 s, as a function of the dose.

The electrical parameters of N-implanted and annealed ZnO:Ga thin films are listed in Table 1. It was found that the annealing parameters had a profound impact on the electrical properties of the film. The resistivity fell and the carrier mobility increased after annealing in O_2 at 550 °C for 30 min, but all samples were *n*-type as determined by room temperature Hall-effect measurements. These outcome can arise from the activation of gallium atoms that move from interstitial to Zn sites and become effective surplus donors to the native donors in ZnO [10,11]. The conversion of the conduction type from *n*- to *p*-type was not observed in N_2 annealed samples either, when the annealing was performed at 550 °C for a reduced time of 10 s. As observed from other groups [12,13], the low temperatures are more favorable for nitrogen incorporation in the ZnO lattice. Therefore, next annealing experiments have been carried out in N_2 atmosphere at 400 for 10 s. The resistivity of the N-implanted ZnO:Ga films increased after annealing in N_2 at 400 °C for 10 s compared to the resistivity of the films annealed in O_2 at 550 °C (Fig. 1). The electron concentration did not change significantly while their mobility decreased more than one order of magnitude (Tab. 1), most likely due to the structural defects that could not be completely removed at the lower annealing temperature. The carrier mobility depends on the scattering events that take place inside the semiconductor. In case of polycrystalline and other high defect materials,

Table 1. Dependence of the properties of N-implanted ZnO:Ga films on the annealing treatment.

Dose (cm^{-2})	Annealing conditions	Resistivity (Ω cm)	Concentration (cm^{-3})	Mobility (cm^2/V s)	Type	Transmittance (%)
1×10^{15}	N_2, 400 °C, 10 s	0.1	1×10^{20}	0,5	n	83
	O_2, 550 °C, 30 min	3.5×10^{-3}	7.6×10^{19}	23	n	87
5×10^{15}	N_2, 400 °C, 10 s	0.16	5×10^{19}	0.7	n	85
	O_2, 550 °C, 30 min	4×10^{-3}	6.4×10^{19}	23	n	87
1×10^{16}	N_2, 400 °C, 10 s	0.46	2.8×10^{19}	0.6	p	90
	O_2, 550 °C, 30 min	4.8×10^{-3}	6×10^{19}	21	n	87
2×10^{16}	N_2, 400 °C, 10 s	0.23	9×10^{19}	0.3	n	84
	N_2, 550 °C, 10 s	4.3×10^{-3}	1.4×10^{20}	11	n	85
	O_2, 550 °C, 30 min	5.8×10^{-3}	5.1×10^{19}	21	n	87

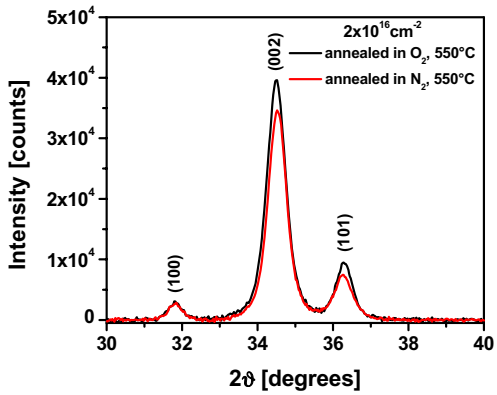

Fig. 2. X-ray diffraction patterns of ZnO:Ga films implanted with 2×10^{16} cm^{-2}, annealed in O_2 at 550 °C for 30 min and N_2 at 550 °C for 10 s.

ionized impurity scattering and scattering by neutral impurity atoms and defects tend to dominate. Impurities and defects can alter the physical parameters of semiconductors and, in some case, can dominate these parameters. At low annealing temperatures, some impurity atoms remain on interstitial positions. Elevating the annealing temperature can activate some of the impurity gallium atoms to move from interstitial to Zn sites, making them effective donors, and/or some of the interstitial impurity nitrogen atoms to substitute for an O atom, thus, becoming acceptors. Hence, with increasing annealing temperature, scattering by neutral impurity atoms and defects decreases, which causes the increase in mobility. The simultaneous formation of donors and acceptors, and prevalence of the first ones, can explain n-type conductivity of the film. The conductivity type was converted to p-type (hole concentration of 2.8×10^{19} cm^{-3}, mobility of 0.6 cm^2/V s, resistivity of 0.46 Ω cm) in the sample implanted with a 1×10^{16} cm^{-2} dose. This result suggests that low temperature treatment can be more favorable for p-type doping in ZnO:Ga films [6], but it is not sufficient to claim the preparation of p-type ZnO.

The dominant (002) diffraction line in the XRD patterns of N-implanted ZnO:Ga films annealed in O_2 and N_2 atmosphere at 550 °C (Fig. 2), shows that these films are preferentially c-axis oriented. The post-implantation annealing reduced the structure damage. The higher integrated intensity of a (002) diffraction line suggests more textured structure after annealing in O_2 for 30 min than after annealing in N_2 for 10 s. The peaks' positions are shifted toward higher 2θ angles and their values for the corresponding diffraction lines are as follow: 31.79°/(100), 34.47°/(002), and 36.27°/(101). A shift to higher 2θ angles corresponds to the reduction of the interplanar spacing d most likely due to Ga atoms that occupy the Zn lattice site. This assumption is supported from the rise in the carrier concentrations, 4×10^{17} $cm^{-3} \div 5.1 \times 10^{19}$ cm^{-3} after a post-implantation annealing in O_2 (550 °C, 30 min), and 8×10^{19} $cm^{-3} \div 1.4 \times 10^{20}$ cm^{-3} after a N_2 anneal (550 °C, 10 s). These results demonstrate the relationship between structural and electrical properties. The reduction of the interplanar spacing will introduce tensile strains (stress) into the film. The biaxial lattice stress is given by the formula [14]

$$\sigma_1 + \sigma_2 = -\frac{E}{\mu}\frac{d - d_0}{d_0} \tag{1}$$

where E is Young's modulus, μ is Poisson's ratio, d_0 is the reference strain-free interplanar spacing and d is the interplanar spacing obtained from the experiment. In Figure 3 are compared stresses from a (002) line for annealing in O_2 and N_2 at 550 °C. It can be seen that annealing in O_2 is more favorable with regard to the film crystalline structure quality. Other authors reported the similar observations [15]. Depending on the annealing conditions, the estimated crystallite size in the films doped with a 2×10^{16} cm^{-2} dose increased, 25 nm (not-annealed), 31 nm (annealed in O_2 at 550 °C for 30 min) and 42 nm (annealed in N_2 at 550 °C for 10 s). The crystallite size was estimated using the Scherrer's formula:

$$\langle D \rangle = \frac{K\lambda}{\beta_C^f \cos\Theta} \tag{2}$$

where $K = 2\sqrt{\ln 2/\pi} \approx 0.94$ is the Scherrer's constant, λ is the wavelength of the X-rays used, β_C^f is the pure (physical) Cauchy component of integral breadth of the line taken in radians and Θ is the Bragg's angle [16].

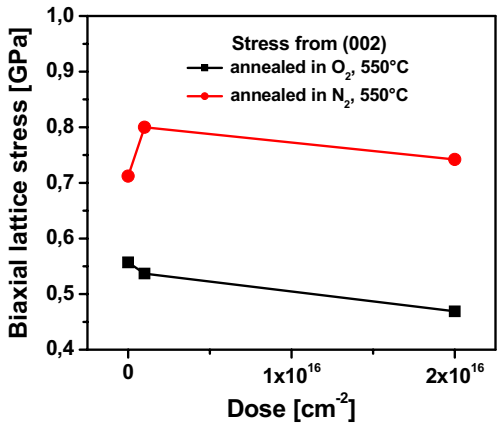

Fig. 3. A biaxial lattice stress from a (002) diffraction line as a function of the dose for N-implanted ZnO:Ga films, annealed in O_2 at 550 °C for 30 min, and annealed in N_2 at 550 °C for 10 s.

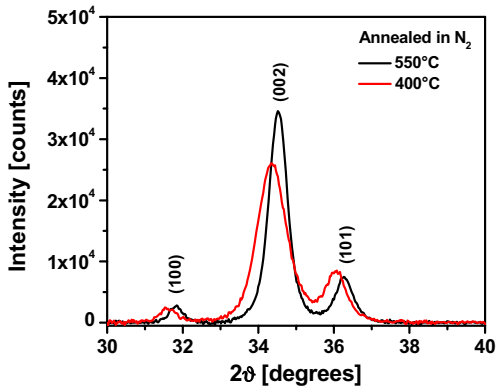

Fig. 4. X-ray diffraction patterns of ZnO:Ga films implanted with 1×10^{16} cm^{-2}, annealed in N_2 at 400 and 550 °C.

The integrated intensity decreased and the diffraction lines position shifts toward lower 2θ diffraction angles after annealing in N_2 at 400 °C (Fig. 4). According to the Bragg's law, the reduction of the diffraction angle corresponds to a lattice expansion and an increase of the interplanar spacing d that introduces compressive stress into the film. These structure changes can arise from N atoms that occupy O sites and create N_O acceptors, and/or other nitrogen related defects and defect complexes in the ZnO lattice. Since, the incorporation of nitrogen atoms into ZnO is more effective at low temperatures [12], the low temperature range may provide better conditions for p-type doping in ZnO. However, it caused the lattice deformation due to the formation of nitrogen related defects in addition to other interstitial and substitution defects that remain after a low temperature anneal.

Implantation and diffusion behavior of nitrogen in the sputtered ZnO:Ga thin films were studied through secondary ion mass spectrometry measurements of non-implanted and N-implanted ZnO:Ga films, before and after annealing treatment. Nitrogen in ZnO is evaluated by monitoring of complex $^{30}NO^-$ ions. The depth profiles of

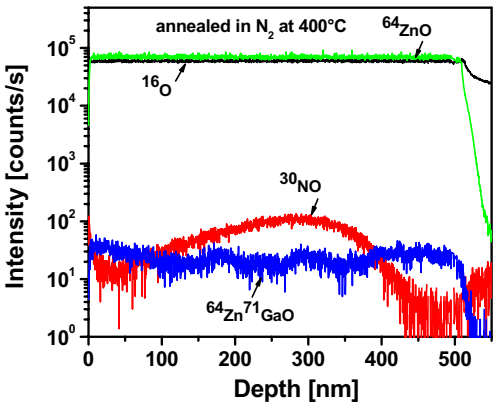

Fig. 5. SIMS depth profiles of N-implanted ZnO:Ga films annealed in N_2 at 400 °C for 10 s.

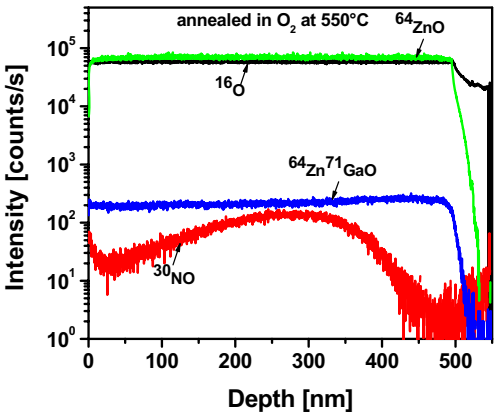

Fig. 6. SIMS depth profiles of N-implanted ZnO:Ga films annealed in O_2 at 550 °C for 30 min.

$^{30}NO^-$ before and after annealing are roughly Gaussian and the depth of the concentration peak is close to the calculated value of the projected range (∼340 nm) obtained by SRIM. The depth profile of the complex $^{30}NO^-$ ions in a p-type film obtained after annealing under N_2 at 400 °C for 10 s is plotted in Figure 5. Figure 6 shows the depth profiles of the negative ions in an n-type film after annealing under O_2 at 550 °C for 30 min. In addition to ^{64}ZnO, ^{16}O and $^{30}NO^-$, all samples contain considerable amounts of $^{64}Zn^{71}GaO$ that can be a source of Ga impurities and n-type conductivity, since Ga is a donor in ZnO. It can be seen that annealing in N_2 at 400 °C caused $^{64}Zn^{71}GaO$ redistribution and its reduction that may be the reason for p-type conductivity in this film. The SIMS results make it clear that the performed annealing treatments under oxygen or nitrogen, at chosen temperatures and times, do not lead to the uniform distribution of the nitrogen impurity in the film. It is in agreement with other authors' observations, which have denoted nitrogen as a less diffusible element in ZnO [17,18]. Hence, the implanted film can be considered a double-layer structure, which can influence the determination of the sign of the Hall coefficient, and the conduction type [19].

In Figure 7 are compared the optical transmittance spectra (including the glass substrate) of the as deposited

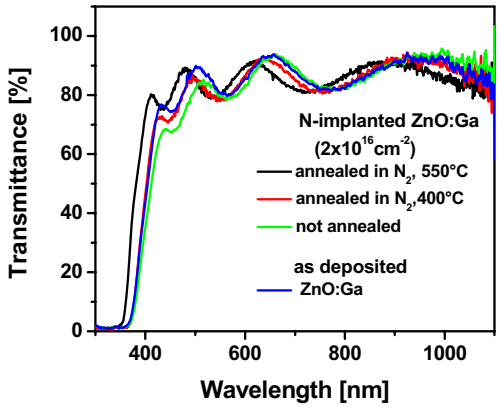

Fig. 7. Optical transmittance spectra of: (a) as deposited ZnO:Ga films (blue line), and N-implanted ZnO:Ga films (implant dose of 2×10^{16} cm^{-2}) (b) not annealed (green line); (c) annealed in N_2 at 400 for 10 s (red line); (c) annealed in N_2 at 550 for 10 s (black line).

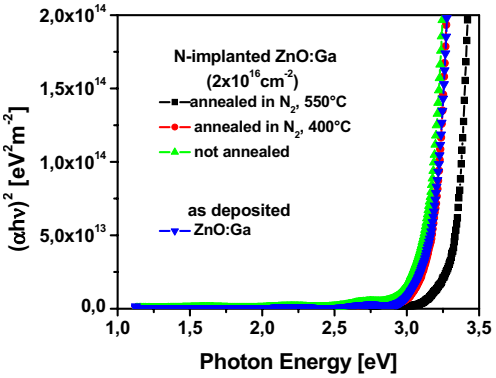

Fig. 8. Plot of the absorption squared $(\alpha h\nu)^2$ versus phonon energy for (a) as deposited ZnO:Ga films (blue line), and N-implanted ZnO:Ga films (implant dose of 2×10^{16} cm^{-2}) (b) not annealed (green line); (c) annealed in N_2 at 400 for 10 s (red line); (c) annealed in N_2 at 550 for 10 s (black line).

ZnO:Ga films and N-implanted ZnO:Ga films (implant dose of 2×10^{16} cm^{-2}), not annealed and annealed in N_2 at 400 and 550 °C for 10 s. The transmittance data were acquired over the wavelength range of $200 < \lambda < 1100$ nm. The optical transmittance depends on both, the implant dose and the annealing conditions (an ambient, time and temperature). All N-implanted films are highly transparent with an average transmittance >84% in the wavelength range of 390–1100 nm. Average transmittance of 87% that was obtained after annealing in O_2 at 550 °C resulted from a better film crystallinity. For the samples annealed in N_2, average transmittance increased from 84 to 85% as annealing temperature was increased from 400 to 550 °C.

The transmittance data were used to calculate the absorption coefficients and to determine the optical band gap of the N-implanted ZnO:Ga films. ZnO is known as a direct band gap material therefore, the direct electron transition from valence to conduction bands was assumed for these calculations. The absorption coefficient was calculated by the following equation:

$$\alpha = \frac{1}{t} \ln \frac{1}{T} \tag{3}$$

where t is the thickness of the film and T is the transmittance. The optical band gap, for allowed direct transitions, can be expressed by the equation [20]:

$$\alpha h\nu = A \left(h\nu - E_g\right)^{1/2} \tag{4}$$

where $h\nu$ is a photon energy, E_g is an optical band gap and A is a constant. The square of the absorption coefficient against photon energy is plotted in Figure 8 for as deposited ZnO:Ga films, and N-implanted ZnO:Ga films (implant dose of 2×10^{16} cm^{-2}), not annealed and annealed in N_2 at 400 and 550 °C for 10 s. The optical band gap of the films was estimated by extrapolating the linear portion of each curve. The optical band gap of the not annealed N-implanted ZnO:Ga film is ∼3.19 eV. Annealing caused widening of the optical band gap. The films annealed in N_2 atmosphere at 400 °C exhibited an optical band gap of 3.23 eV, which widen to 3.3 eV after annealing at 550 °C.

4 Conclusion

The sputtered ZnO:Ga thin films were implanted with 180 keV N ions with the doses ranging from 1×10^{15} to 2×10^{16} cm^{-2}. The SIMS depth profiles of the complex $^{30}NO^-$ ions before and after annealing are roughly Gaussian and the depth of the concentration peak is close to the calculated value of the projected range obtained by SRIM. The non-implanted ZnO:Ga films were n-type conductivity with the electron concentration in the range of 5×10^{19}–7.2×10^{19} cm^{-3} and a c-axis preferred orientation of the crystallites. It was found that the annealing conditions had a profound impact on the film properties. The resistivity of the films increased after nitrogen implantation and it decreased significantly after post-implantation annealing under both O_2 and N_2 ambient at 550 °C. Lower temperature annealing in N_2 at 400 °C caused the rise in resistivity mainly as a result from the reduction in mobility. The conductivity type was converted to p-type (hole concentration of 2.8×10^{19} cm^{-3}, mobility of 0.6 cm^2/V s, resistivity of 0.46 Ω cm) in the sample implanted with a 1×10^{16} cm^{-2} dose, suggesting that annealing at low temperatures can be more favorable for obtaining p-type ZnO:Ga films via nitrogen implantation. The dominant (002) diffraction line in the XRD patterns of all N-implanted and annealed ZnO:Ga films shows that these films have a c-axis preferred orientation of the crystallites. The correlation was found between the annealing conditions and the microstructure, electrical and optical properties of these films. Post-implantation annealing reduces the structure damages and biaxial lattice stresses. The transition from compressive to tensile stress was observed after annealing in O_2 and N_2 at 550 °C. Hence, the carrier concentration increased (4×10^{17} cm$^{-3} \div 5.1 \times 10^{19}$ cm^{-3}), resistivity decreased and average transmittance of 87%

was obtained after post-implantation annealing in O_2 at 550 °C. These results are consistent with the shift of the band edge to lower wavelengths and the band gap widening. The films were under compressive stress and had higher resistivity due to nitrogen incorporation and formation of N_O acceptors after annealing in N_2 at 400 °C.

Presented work was supported by the the CENTEM project, reg. No. CZ.1.05/2.1.00/03.0088 cofunded from the ERDF the OP RDI programe of the MEYS CR within the project No. 1M06031, the APVV project LPP-0094-09 and SK-SRB-0012-09 and the SK Grant Agency VEGA project 1/0220/09. Support from the Serbian Ministry of Science and Technological Development (Project 171023) and the EU FP7 Project SPIRIT are also acknowledged.

References

1. H. Liu, V. Avrutin, N. Izyumskaya, Ü. Özgür, H. Morkoç, Superlatt. Microstruct. **48**, 458 (2010)
2. S.-H.K. Park, J.-I. Lee, C.-S. Hwang, H.Y. Chuj, Jpn J. Appl. Phys. **44**, L242 (2005)
3. R.L. Hoffman, B.J. Norris, J.F. Wager, Appl. Phys. Lett. **82**, 733 (2003)
4. X. Li, S.E. Asher, S. Limpijumnong, B.M. Keyes, C.L. Perkins, T.M. Barnes, H.R. Moutinho, J.M. Luther, S.B. Zhang, S.-H. Wei, T.J. Coutts, J. Cryst. Growth **287**, 94 (2006)
5. V. Tvarozek, K. Shtereva, I. Novotny, J. Kovac, P. Sutta, R. Srnanek, A. Vincze, Vacuum **82**, 166 (2008)
6. A.N. Georgobiani, A.N. Gruzintsev, V.T. Volkov, M.O. Vorobiev, V.I. Demin, V.A. Dravin, Nucl. Instrum. Meth. Phys. Res. A **514**, 117 (2003)
7. Ch.-Ch. Lin, S.-Y. Chen, S.-Y. Cheng, H.-Y. Lee, Appl. Phys. Lett. **84**, 5040 (2004)
8. M. Milosavljević, D. Peruško, V.Milinović, P. Gašpierik, I. Novotný, V. Tvarožek, in *Proceedings of 8th International Conference on Advanced Semiconductor Devices & Microsystems*, *Smolenice, Slovak Republic*, edited by J. Breza, D. Donoval, E. Vavrinsky (2010), p. 183
9. E.Ch. Lee, Y.S. Kim, Y.G. Jin, K.J. Chang, Physica B **912**, 308 (2001)
10. V. Khranovskyy, U. Grossner, V. Lazorenko, G. Lashkarev, B.G. Svensson, R. Yakimova, Superlatt. Microstruct. **42**, 379 (2007)
11. X. Yu, J. Ma, F. Ji, Y. Wang, X. Zhang, H. Ma, Thin Solid Films **483,** 296 (2005)
12. S.H. Park, J.H. Chang, H.J. Ko, T. Minegishi, J.S. Park, I.H. Im, M. Ito, D.C. Oh, M.W. Cho, T. Yao, Appl. Surf. Sci. **254**, 7972 (2008)
13. K. Nakahara, H. Takasu, P. Fons, A. Yamada, K. Iwata, K. Matsubara, R. Hunger, S. Niki, J. Cryst. Growth **237–239**, 503 (2002)
14. P. Šutta, Q. Jackuliak, in *Proceedings of 2nd International Conference on Advanced Semiconductor Devices & Microsystems*, *Smolenice, Slovak Republic*, edited by J. Breza (1998), p. 227
15. Ch.-Ch. Yang, Ch.-Ch. Lin, Ch.-H. Peng, S.-Y. Chen, J. Cryst. Growth **285**, 96 (2005)
16. R. Delhez, Th.H. de Keijser, E.J. Mittemeijer, Z. Fresenius, Anal. Chem. **312**, 1 (1982)
17. D.-Ch. Park, I. Sakaguchi, N. Ohashi, Sh. Hishita, H. Haneda, Appl. Surf. Sci. **203-204**, 359 (2003)
18. J. Lee, J. Metson, P.J. Evans, U. Pal D. Bhattacharyya, Appl. Surf. Sci. **256**, 2143 (2010)
19. V. Vaithianathan, Sh. Hishita, J.H. Moon, S.S. Kim, Thin Solid Films **515**, 6927 (2007)
20. S.M. Sze, in *Physics of Semiconductor Devices*, 2nd edn. (John Wiley & Sons, Inc., New York, 1981), p. 72